

1
2
3
4
5
6
7
8
9
10
11
12
13
14
15
16
17
18
19
20
21
22
23
24
25
26
27
28
29
30
31
32
33

Supplementary Information for

**Negative Pressure Membrane Distillation for Excellent
Gypsum Scaling Resistance and Flux Enhancement**

Yongjie Liu^{a,b}, Thomas Horseman^c, Zhangxin Wang^{d,e}, Hassan A. Arafat^b, Huabing Yin^f,
Shihong Lin^{c,g,*}, Tao He^{a,*}

- a. Shanghai Advanced Research Institute, Chinese Academy of Sciences, Shanghai 201210, China
- b. Center for Membrane and Advanced Water Technology, Khalifa University, Abu Dhabi, United Arab Emirates
- c. Department of Chemical and Biomolecular Engineering, Vanderbilt University, Nashville, Tennessee 37235-1831, United States
- d. Key Laboratory for City Cluster Environmental Safety and Green Development of the Ministry of Education, Institute of Environmental and Ecological Engineering, Guangdong University of Technology, Guangzhou, 510006, China
- e. Guangdong Provincial Key Laboratory of Water Quality Improvement and Ecological Restoration for Watershed, Institute of Environmental and Ecological Engineering, Guangdong University of Technology, Guangzhou, 510006, China
- f. School of Engineering, University of Glasgow, Glasgow, G12 8LT, UK
- g. Department of Civil and Environmental Engineering, Vanderbilt University, Nashville, Tennessee 37235-1831, United States

*Corresponding authors:
Shihong Lin shihong.lin@vanderbilt.edu Tao He het@sari.ac.cn

Contents:
19 Pages
3 Supporting Table
4 Supporting Figures

34 **Section S1:** Experimental details for membrane characterization and performance test

35 **S1.1 Pore size measurement**

36 Pore size was conducted with Capillary Flow Porometry (Porolux 1000, POROMETER,
37 Belgium). The membrane was pre-wetted with commercial low surface tension liquid Porefil
38 (surface tension: 16 dyne/cm). After mounting the sample onto the test cell, the measurement
39 was managed with a program consisting of wet-run and dry-run. The wet-run was realized by
40 replacing the wetting liquid within a certain pore size by compressed air at certain pressure
41 until the membrane was dried out (wet-run). Then the air flow rate of the membrane was tested
42 by decreasing the air pressure (dry-run). The bubble point was determined as the pressure at
43 which significant flow of air was detected.

44 **S1.2 Water contact angle and sliding angle**

45 Water contact and sliding angles were measured by a contact angle goniometer (Drop
46 Meter A-100P, MAIST, Ningbo, China) equipped with a high-speed CCD camera. A water
47 droplet of 5 μL was deposited on the membrane surface for contact angle measurements, and
48 each reported value was the average of five measurements.

49 **S1.3 Liquid entry pressure**

50 Liquid entry pressure (LEP) is a measure of the ability of a hydrophobic membrane to
51 resist pore wetting. LEP was measured using a dead-end filtration set-up with deionized water.
52 Pressure on the feed side was increased stepwise while allowing it to stabilize for a couple of
53 minutes after each increment (0.05 bar). The pressure at which the first water droplet gets
54 through the membrane is taken as the LEP.

55 **S1.4 Preparation of CF_4 -MP-PVDF membrane**

56 A custom-made PDMS mold was created using a silicon wafer with a micro-pillar

57 structure as a complimentary structure. It was then utilized in a non-solvent induced phase
 58 separation (NIPS) process to make a micro pillared PVDF membrane (MP-PVDF). Using the
 59 plasma treatment technology, CF₄ plasma treatment was used to improve the hydrophobicity
 60 of the MP-PVDF (IoN40, PVA Tepla Co. Ltd). The membrane was pretreated with argon
 61 plasma at 45 W/15 s and CF₄ plasma at a glow discharge of 200 W/15 min, to summarize.
 62 CF₄-MP-PVDF denoted the name of final membrane.

63 **S1.5 Pulse flow membrane distillation**


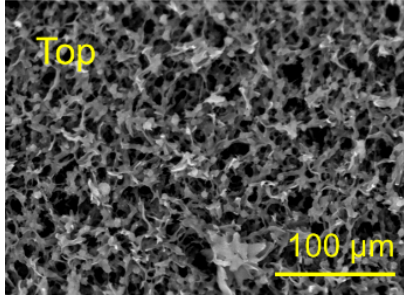
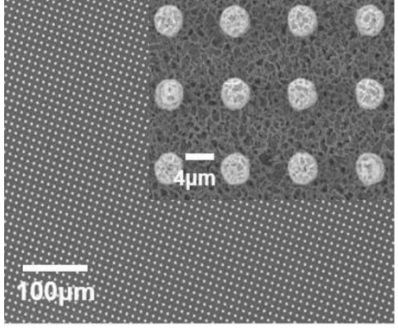
64 Detailed description of the pulse flow MD experiments can be found in our previous
 65 publication.¹ Briefly, a bench-scale direct contact membrane distillation unit was developed to
 66 assess the scaling behavior of peristaltic pumps with the pulse. In the feed side, the peristaltic
 67 pump revolves at 56 rpm, resulting in a frequency of 2.8 Hz (56 r/min and three pulses per
 68 rotation). The other operation conditions were same with NP-DCMD experiment.

69

70

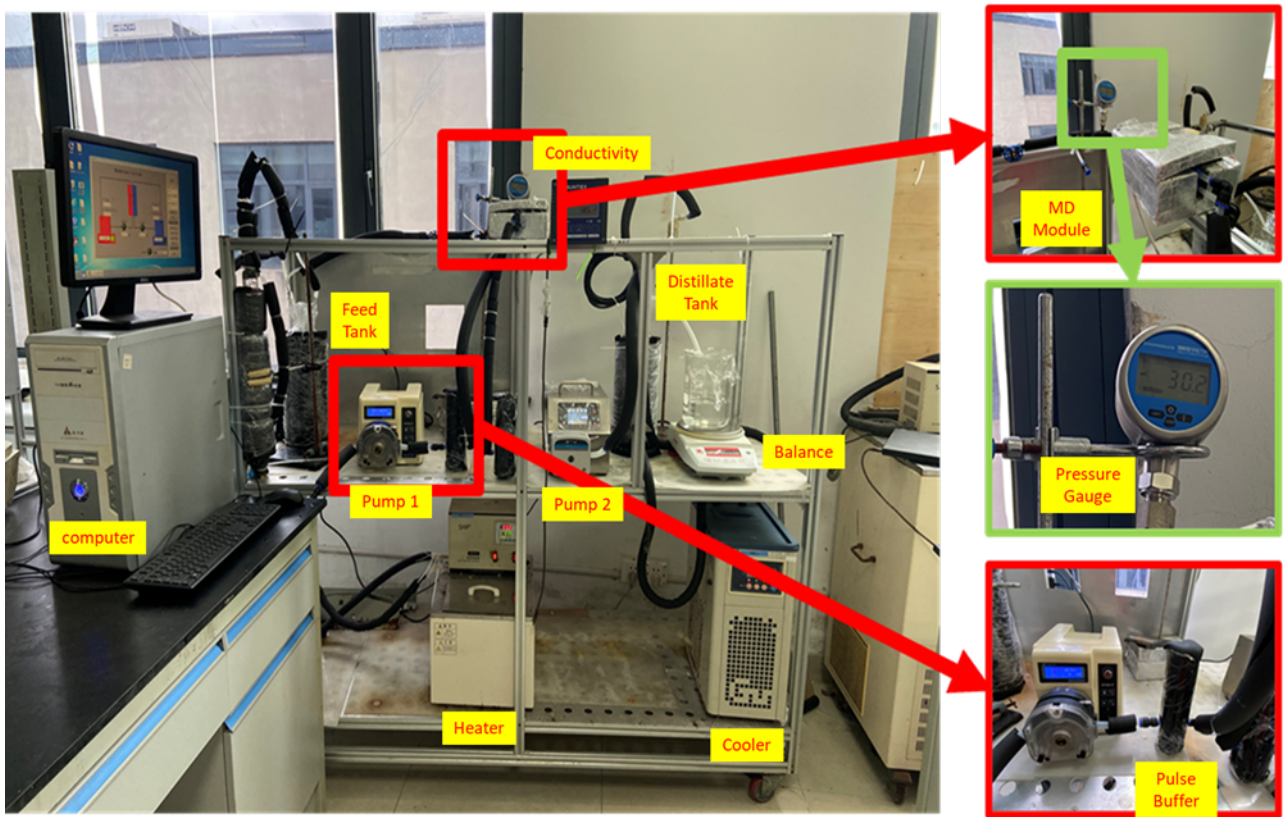
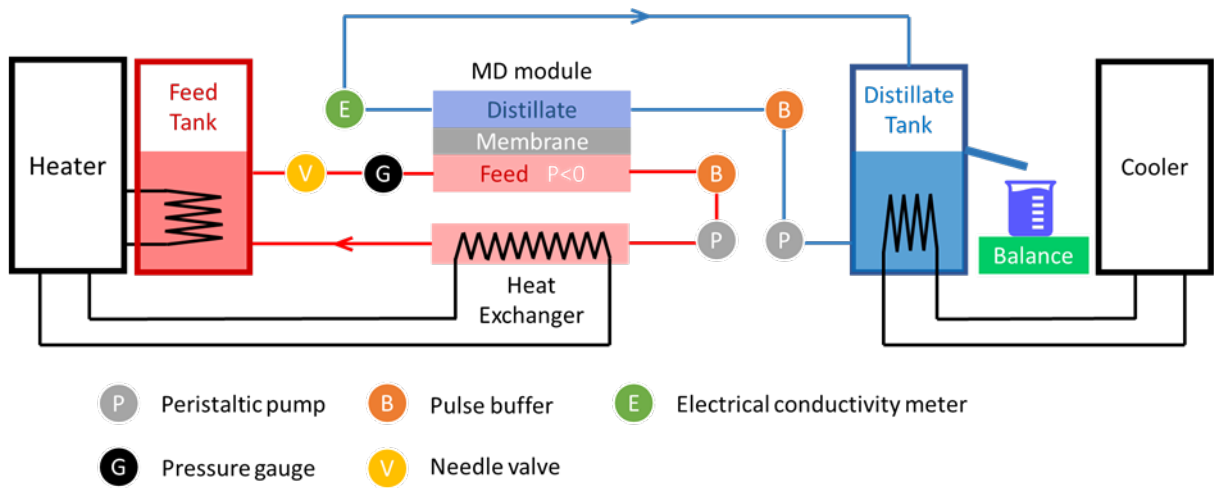
71 **Table S1** Characteristics of the commercial PVDF membrane and CF₄-MP-PVDF. *

membrane	Commercial PVDF (GVHP00010)	CF ₄ -MP-PVDF
Thickness (μm)	125	264
Mean flow pore size (μm)	0.22	0.20
Contact angle (°)	110	166.8

Sliding angle (°)		3.0
Porosity (%)	75	79
LEP (bar)	2.4	/
SEM image		

72 * The results of CF4-MP-PVDF is obtained from our previous work ².

73



74

75 **Figure S1:** Schematic and photographic image and of the DCMD experimental setup.

76

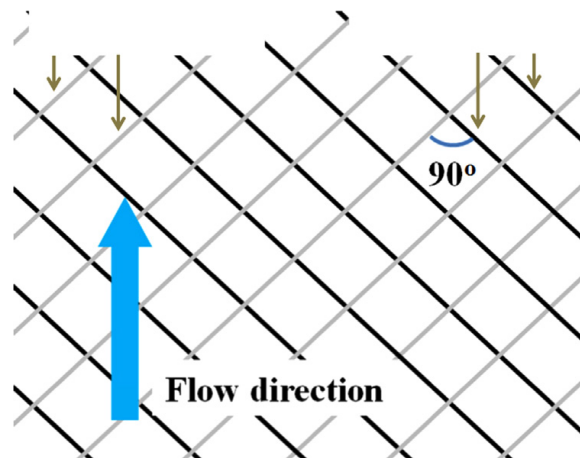
77 **Table S2 Pressures outside the MD cell (measured) and in the feed channel (estimated using**
78 **Bernoulli equation).** Diameters of tubing and equivalent diameter of feed channel are 6 and
79 10.3 mm respectively. Correspondingly, the flow velocities are 0.354 and 0.120 m/s in the
80 tubing and feed channel, respectively. The difference in flow velocities contributes to a
81 pressure difference of ~0.055 kPa (larger in feed channel) based on Bernoulli equation.
82

Pressure measured in the tubing (kPa)	Calculated pressure in the feed channel (kPa)
1	1.06
-10	-9.94
-20	-19.94
-30	-29.94

83

84

85

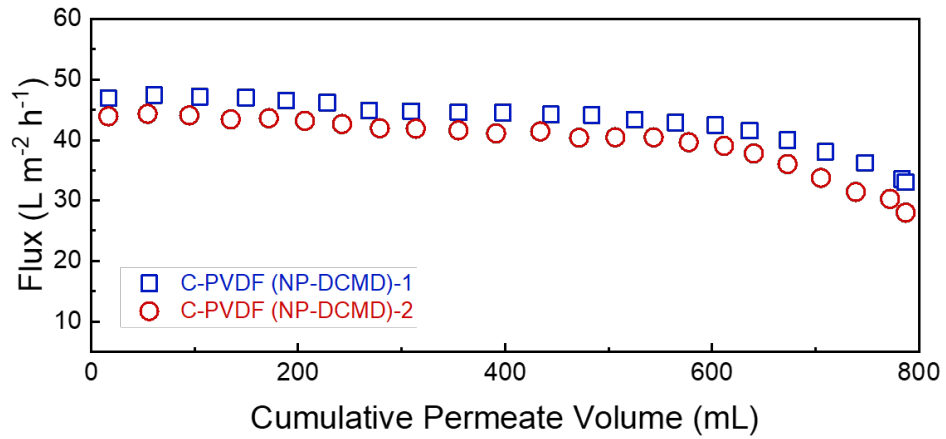


86

87

88

Figure S2. Schematic illustration of the spacer structure. The arrow indicates flow direction. ³



89

90 **Figure S3.** Replicate data of NP-DCMD experiment with a feed solution containing 2000 ppm
 91 CaSO_4 . The feed solution contained 2000 mg L^{-1} CaSO_4 solution (saturation index, $\text{SI}=0.09$).
 92 The temperatures of the feed solution and distillate were 70 °C and 20 °C, respectively. The
 93 same crossflow velocity of 0.17 m/s was used in both the feed and distillate streams. The
 94 experiments were stopped when the cumulative distillate volume reached 800 mL because the
 95 feed volume became insufficient for flow circulation.

96

97

98 **Section S2: Vapor transport in MD**

99 The resistances for the Knudsen flow (R_k) and molecular diffusion (R_{md}) can be
 100 estimated using equations 2.1 and 2.2, respectively:⁴

$$101 \quad R_k = \left[\frac{2}{3} \frac{\varepsilon r}{\tau \delta} \left(\frac{8M}{\pi RT_m} \right)^{0.5} \right]^{-1} \quad (2.1)$$

102 and

$$103 \quad R_{md} = \left[\frac{\varepsilon}{\tau \delta} \frac{PD}{P_a} \frac{M}{RT_m} \right]^{-1} \quad (2.2)$$

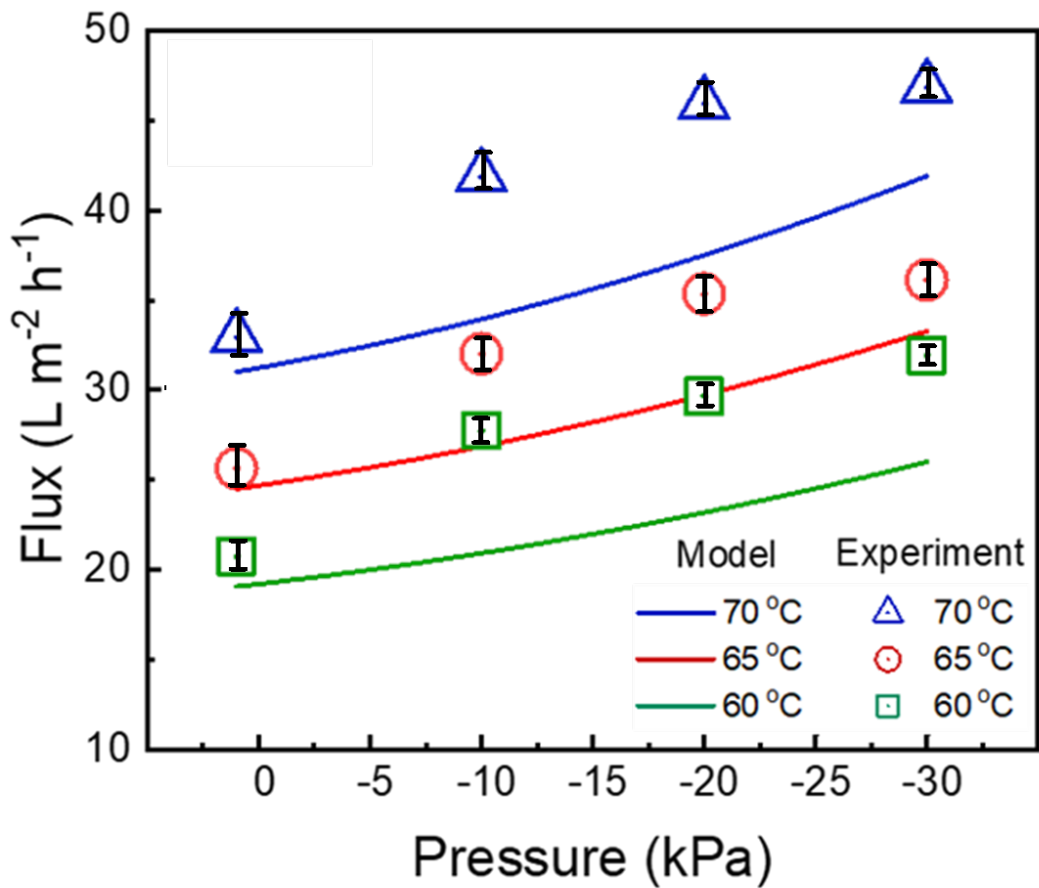
104 Where ε , τ and r are the membrane porosity, pore tortuosity and pore radius, respectively, M
 105 is the molecular weight of water molecule, R is the ideal gas constant and T_m is the
 106 temperature inside the membrane pores, which can be assumed as the average of the
 107 temperatures of the membrane surface at feed and distillate sides, P_a and P are the air pressure
 108 and the total pressure inside the pore and D is the diffusion coefficient of water vapor
 109 molecules. We note that PD is function of temperature.⁵ Integrating R_k and R_{md} yields the
 110 membrane permeability coefficient, B_m :

$$111 \quad B_m = \left[\frac{1}{R_k} + \frac{1}{R_{md}} \right]^{-1} \quad (2.3)$$

112 The water flux J through the membrane can be calculated by multiplying B_m and the driving
 113 force for vapor transfer, i.e., the difference of saturated water vapor pressure at the feed-
 114 membrane interface, $P_{m,f}$, and that at the distillate-membrane, $P_{m,d}$:

$$115 \quad J = B_m (P_{m,f} - P_{m,d}) \quad (2.4)$$

116



117

118 **Figure S4.** Vapor flux as functions of feed gauge pressure (1.0 kPa to -30 kPa) at different
 119 feed temperatures (60, 65 and 70 °C). The symbols represent experimental data whereas the
 120 curves represent simulation results based on the Dusty-Gas model. The gauge pressure and
 121 temperature of the distillate were fixed at 0.1 kPa and 20 °C, respectively. The experimental
 122 results are also reported in Table S3.

123

124 **Table S3** Mean value (and standard deviation) water flux under different temperature and
125 pressures.

<i>Pressure (kPa)</i>	<i>Temperature (°C)</i>		
	60	65	70
<i>1</i>	20.74 (0.78)	23.86 (1.10)	32.94 (1.17)
<i>-10</i>	27.75 (0.67)	33.61 (0.88)	41.89 (1.00)
<i>-20</i>	29.66 (0.61)	35.46 (0.98)	44.94 (0.91)
<i>-30</i>	31.93 (0.51)	37.51 (0.89)	46.84 (0.76)

126
127

128 **Section S3: Detailed description of heat transfer in MD**

129 At steady state, the overall heat flux from the hot feed to the cold distillate side, q , is
130 given by:

$$131 \quad q = q_f = q_m = q_d \quad (3.1)$$

132 where q_f and q_d are the convective heat fluxes through the feed and distillate boundary layers,
133 respectively, and q_m is the heat flux across the membrane.

134 The convective heat fluxes through the feed and distillate boundary layers are
135 calculated based on the temperature gradient between the bulk (T_b) and membrane surface
136 (T_m) temperatures:

$$137 \quad q_f = h_f (T_{b,f} - T_{m,f}) \quad (3.2)$$

138 And

$$139 \quad q_d = h_d (T_{m,d} - T_{b,d}) \quad (3.3)$$

140 where h is the convective heat transfer coefficient in the boundary layer and the subscript f
141 and d denote the feed and distillate side, respectively. $T_{b,f}$ and $T_{b,d}$ were estimated as the
142 average of the inlet and outlet temperatures on each respective side of the membrane.

143 The heat flux across the membrane consists of both the conductive heat transfer through
144 the membrane and the heat transferred via the latent heat of evaporation, ΔH_{vap} , as follows:

$$145 \quad q_m = h_m (T_{m,f} - T_{m,d}) + J \Delta H_{vap} \quad (3.4)$$

146 where h_m is the overall conductive heat transfer coefficient of the membrane. The first part on
147 the left side in equation 3.4 represent the conductive heat flux through the membrane (Q_c)
148 while the second part represents the heat transferred via evaporation (Q_v). We note that Q_v is
149 a favorable as it results from vapor flux (i.e., water production), whereas Q_c represents an

150 unfavorable heat transfer that leads to a loss of driving force. The overall conductive heat
 151 transfer coefficient, h_m , is calculated from the thermal conductivities of the membrane polymer,
 152 k_m , and the trapped air inside the pores, k_g as follows:

$$153 \quad h_m = \frac{k_g \varepsilon + k_m (1 - \varepsilon)}{\delta} \quad (3.5)$$

154 where δ is the membrane thickness. The thermal efficiency (η , %) of the DCMD system is
 155 the ratio between the heat flux due to vapor transfer and the total heat flux (i.e., the sum of heat
 156 fluxes due to both vapor transfer and conductive heat transfer):

$$157 \quad \eta = \frac{Q_v}{Q_c + Q_v} \times 100\% \quad (3.6)$$

158 Under positive feed pressure, the feed stream will have stagnant zones due to the convex
 159 liquid-gas interface partially wetting the pores near the surface and a non-slip boundary can be
 160 assumed at the membrane surface. However, in NP-DCMD, the liquid-gas interface is concave
 161 because the air inside the pores expands when negative feed pressure is applied, thus enhancing
 162 the flow hydrodynamics (by eliminating the stagnant zones) and increasing the flow due to
 163 slip-boundary condition at the liquid-gas interface (i.e., the feed velocity at the interface is not
 164 zero). To account for that, h_f was multiplied with a new factor, φ_1 . Moreover, because of the
 165 concaved liquid-gas interface, the liquid-solid contact area decreases, and the evaporation area
 166 increases, which has an impact on the actual free pore volume within the membrane and,
 167 consequently, on h_m (equation 3.5). To account for this, h_m was multiplied by a second factor,
 168 φ_2 . As a result, equations 3.2 and 3.4 are modified as follows:

$$169 \quad q_f = \varphi_1 h_f (T_{b,f} - T_{m,f}) \quad (3.7)$$

170 and

171
$$q_m = \phi_2 h_m (T_{m,f} - T_{m,p}) + J \Delta H_{vap} \quad (3.8)$$

172 The model calculation process involves combining mass and heat transfer, as detailed in our

173 previous paper.⁶ The MATLAB code for the calculations is provided in the following **S4**.

174

```

175 Section S4: MATLAB code of mass and heat transfer in NP-DCMD
176 %% NP-DCMD Flux Prediction Program Version 5
177 % Update Date: 11/10/2021
178 % Written by Yongjie Liu (Email: liu.yong-jie@outlook.com; 100058656@ku.ac.ae)
179
180 %% The seawater thermophysical performance was obtained from
181 http://web.mit.edu/seawater/.
182 %% Before using this code please download the files from
183 http://web.mit.edu/seawater/SEAWATER\_v3.1.4\_20Feb17.zip and decompress all the
184 files in the same folder of this program.
185
186 clear all; close all; clc
187 %% Input Factor for Negative Feed Pressure DCMD
188 P_f = 101325+1000 % Pressure in feed channel [Pa]
189 phi_1 = 1 % Slippery boundary effect [-]
190 phi_2 = 1 % Optimal heat transfer effect [-]
191 T_fin = 60+273.15; % Feed Inlet Temperature [K]
192 T_fout = 59+273.15; % Feed Outlet Temperature [K]
193 T_din = 20+273.15; % distillate Inlet Temperature [K]
194 T_dout = 21+273.15; % distillate Outlet Temperature [K]
195
196 %% Definitions
197 % Constants
198 k_B = 1.381e-23; % Boltzmann constant [J/K]
199 R = 8.314; % Universal gas constant [Pa m^3/mol K]
200
201 % Membrane Parameters
202 mem_prop = 0.75; % membrane porosity [-]
203 mem_thick = 125e-6; % membrane thickness [m]
204 mem_tau = 1.1; % membrane tortuosity [-]
205 mem_pore = 0.22e-6; % membrane pore diameter [m]
206
207 % Membrane Module
208 W = 0.02; % Channel Width [m]
209 L = 0.05; % Channel Length [m]
210 H = 0.003; % Channel Height [m]
211 mem_A = L*W; % Effective membrane surface [m^2]
212 flow_A = H*W; % Area for flow channel [m^2]
213 d_h = 2*W*H/(W+H); % Hydraulic diameter [m]
214
215 % Operation Conditions
216 % Temperature
217 T_f = (T_fin+T_fout)/2; % Average Feed Temperature [K]

```

```

218     T_d = (T_din+T_dout)/2; % Avarage distillate Temperature [K]
219     T_mf_guess = T_f; T_md_guess=T_d;
220
221     % Flow Conditions
222     V_f = 600/1000000/60; % [mL/min]->[m^3/s] Feed flow rate
223     V_d = 600/1000000/60; % [mL/min]->[m^3/s] distillate flow rate
224     u_f = V_f/flow_A; % [m/s] Velocity of feed stream
225     u_d = V_d/flow_A; % [m/s] Velocity of distillate stream
226
227 % Seawater Parameters
228 uT = 'K'; % Unit of Temperature
229 uS = 'ppm'; % Unit of Saline
230 uP = 'Pa'; % Unit of Pressure
231     % Feed Side
232     T = T_f;
233     S = 0; % Saline Concentration [ppm]
234     P = P_f;
235     Pv_f = SW_Psat(T,uT,S,uS); % Saturation pressure of seawater [N/m^2]
236     rho_f = SW_Density(T,uT,S,uS,P,uP); % Density of seawater [kg/m^3]
237     hfg_f = SW_LatentHeat(T,uT,S,uS); % Latent Heat of vaporization of seawater
238 [J/kg]
239     k_f = SW_ConductivityP(T,uT,S,uS,P,uP); % Thermal conductivity of seawater
240 [W/m-K]
241     mu_f = SW_Viscosity(T,uT,S,uS); % Dynamic viscosity of seawater [kg/m-
242 s]
243     cp_f = SW_SpcHeat(T,uT,S,uS,P,uP); % Specific heat of seawater[J/kg-K]
244     % Distillate Side
245     T = T_d;
246     S = 0; % Saline Concentration [ppm]
247     P = 101325+1000;
248     Pv_d = SW_Psat(T,uT,S,uS); % Saturation (vapor) pressure of seawater [N/m^2]
249     rho_d = SW_Density(T,uT,S,uS,P,uP); % Density of seawater [kg/m^3]
250     hfg_d = SW_LatentHeat(T,uT,S,uS); % Latent Heat of vaporization of seawater
251 [J/kg]
252     k_d = SW_ConductivityP(T,uT,S,uS,P,uP); % Thermal conductivity of seawater
253 [W/m-K]
254     mu_d = SW_Viscosity(T,uT,S,uS); % Dynamic viscosity of seawater [kg/m-s]
255     cp_d = SW_SpcHeat(T,uT,S,uS,P,uP); % Specific heat of seawater[J/kg-K]
256
257 %% Loop iteration to calculate
258 eer=1;i=1;
259 while abs(eer)>10^-7
260     % Membrane Thermal Conductivity
261     T_m =(T_mf_guess+T_md_guess)/2; % Avarage Membrane Temperature [K]

```



```

262         k_pvdf_m=5.77e-4*T_m+0.914e-2; % Thermal Conductivity of PVDF [J/m^2-s-K]
263         k_g=1.36e-3+3.885e-5*T_m+1.66e-3*T_m^0.5; % Thermal Conductivity of Gas
264 [J/m^2-s-K]
265         k_m=(1-mem_prop)*k_pvdf_m+mem_prop*k_g; % Thermal Conductivity of Membrane
266 [J/m^2-s-K]
267
268     % Reynolds, Prandtl and Nusselt Numbers
269     % Feed Side
270     Re_f = rho_f*u_f*d_h/mu_f; % Re in Feed [-]
271     Pr_f = cp_f*mu_f/k_f; % Pr in Feed [-]
272     if Re_f > 2300 % Nu in Feed [-]
273         Nu_f = 1.62*(Re_f*Pr_f*d_h/L)^(1/3);
274     else
275         Nu_f = 0.023*Re_f^0.8*Pr_f^(1/3);
276     end
277
278     % Distillate Side
279     Re_d = rho_d*u_d*d_h/mu_d; % Re in Feed [-]
280     Pr_d = cp_d*mu_d/k_d; % Pr in Feed [-]
281     if Re_d > 2300 % Nu in Feed [-]
282         Nu_d = 1.62*(Re_d*Pr_d*d_h/L)^(1/3);
283     else
284         Nu_d = 0.023*Re_d^0.8*Pr_d^(1/3);
285     end
286
287     % Heat Transfer Coefficients
288     h_f=Nu_f*k_f/d_h; % Heat Transfer Coefficient in Feed [J/m^2-s]
289     h_d=Nu_d*k_d/d_h; % Heat Transfer Coefficient in distillate[J/m^2-s]
290     h_m=k_m/mem_thick; % Heat Transfer Coefficient for membrane[J/m^2-s]
291
292
293     % MD mass transfer coefficient
294     CD_a= 364e-12; % Colloined Distance of Air [m]
295     CD_w= 265e-12; %Colloined Distance of Water Vapor [m]
296     M_w = 18e-3; % Molecule Weight of Water [kg/mol]
297     M_a = 28e-3; % Molecule Weight of Air [kg/mol]
298     P_m = P_f; % Pressure in the Membrane [Pa]
299     Pv_mf = SW_Psat(T_mf_guess,uT,S,uS); % Feed Latent Heat of vaporization of
300 seawater [J/kg]
301     Pv_md = SW_Psat(T_md_guess,uT,S,uS); % Distillate Latent Heat of vaporization
302 of seawater [J/kg]
303     P_a = P_m-(Pv_mf+Pv_md)/2; % Average Air Pressure in Membrane [Pa]
304     lamda=k_B*T_m/(P_m*pi*(CD_a+CD_w)^2)*(1+M_w/M_a)^0.5; % Molecular Free Path
305 [m]

```

```

306     Kn=lamda/mem_pore; % Kn
307     Bm_kd=mem_prop*mem_pore/(3*mem_tau*mem_thick)...
308         *(8*M_w/pi/R/T_m)^0.5; % Bm_Knudsen Diffusion[s/m]
309     PD=1.9e-5*T_m^2.072; % PD
310     Bm_mo=mem_prop*PD*M_w/(mem_tau*mem_thick*P_a*R*T_m); % Bm_Molecule
311     Diffusion[s/m]
312     Bm_T=1/(1/Bm_kd+1/Bm_mo); % Bm_kd+mo [s/m]
313     if Kn>1 % Confirm to use which Bm
314         Bm=Bm_kd;
315     else
316         if 0.01<Kn<1
317             Bm=Bm_T;
318         else Kn<0.01
319             Bm=Bm_mo;
320         end
321     end
322     J = Bm*(Pv_mf-Pv_md); % Water Flux [kg/m^2-s]
323
324     % Temperature on Membrane Surface
325     hfg_m = SW_LatentHeat(T_m,uT,S,uS); % Latent Heat of vaporization of seawater
326     T_m [J/kg]
327     Q_d=h_d*(T_md_guess-T_d); % Distillate Heat Flux [J/m^2]
328     Q_mm=phi_2*h_m*(T_mf_guess-T_md_guess); % Membrane material heat flux [J/m^2]
329     Q_w=J*hfg_m; % Water evaporation heat [J/m^2]
330     Q_m=Q_mm+Q_w; % Membrane Heat Flux [J/m^2]
331     eer=Q_d-Q_m; % Error for Q_d and Q_m
332     if eer < 0 % Majorized Iterative Method
333         T_mf=T_mf_guess;
334         T_md=T_md_guess;
335         T_mf_guess=T_mf_guess-i;
336         T_md_guess=phi_1*h_f*(T_f-T_mf_guess)/h_d+T_d;
337     else
338         T_mf=T_mf_guess;
339         T_md=T_md_guess;
340         T_mf_guess=T_mf_guess+i;
341         T_md_guess=phi_1*h_f*(T_f-T_mf_guess)/h_d+T_d;
342         i=i/10
343     end
344
345 end
346
347

```

348 **Reference:**

- 349 1. Liu, Y.; Li, Z.; Xiao, Z.; Yin, H.; Li, X.; He, T., Synergy of slippery surface and pulse flow: An anti-scaling
350 solution for direct contact membrane distillation. *J. Membr. Sci.* **2020**, *603*, 118035.
- 351 2. Xiao, Z.; Zheng, R.; Liu, Y.; He, H.; Yuan, X.; Ji, Y.; Li, D.; Yin, H.; Zhang, Y.; Li, X.-M.; He, T., Slippery for
352 scaling resistance in membrane distillation: A novel porous micropillared superhydrophobic surface.
353 *Water Res.* **2019**, *155*, 152-161.
- 354 3. Yang, C.; Tian, M.; Xie, Y.; Li, X.-M.; Zhao, B.; He, T.; Liu, J., Effective evaporation of CF₄ plasma
355 modified PVDF membranes in direct contact membrane distillation. *J. Membr. Sci.* **2015**, *482*, 25-32.
- 356 4. Ahmed, F. E.; Lalia, B. S.; Hashaikeh, R.; Hilal, N., Alternative heating techniques in membrane
357 distillation: A review. *Desalination* **2020**, *496*.
- 358 5. Cussler, E. L.; Cussler, E. L., *Diffusion: mass transfer in fluid systems*. Cambridge university press:
359 2009.
- 360 6. Khayet, M., Membranes and theoretical modeling of membrane distillation: A review. *Adv. Colloid*
361 *Interface Sci.* **2011**, *164*, (1-2), 56-88.

362